Front. Comput. Sci. China 2011, 5(1): 57–65
DOI 10.1007/s11704-010-0337-3

RESEARCH ARTICLE

A fast algorithm for computing moments of gray images based on NAM and extended shading approach

Yunping ZHENG (✉)[1], Mudar SAREM[2]

1 School of Computer Science and Engineering, South China University of Technology, Guangzhou 510006, China
2 School of Software Engineering, Huazhong University of Science and Technology, Wuhan 430074, China

Abstract Computing moments on images is very important in the fields of image processing and pattern recognition. The non-symmetry and anti-packing model (NAM) is a general pattern representation model that has been developed to help design some efficient image representation methods. In this paper, inspired by the idea of computing moments based on the S-Tree coding (STC) representation and by using the NAM and extended shading (NAMES) approach, we propose a fast algorithm for computing lower order moments based on the NAMES representation, which takes $O(N)$ time where N is the number of NAM blocks. By taking three idiomatic standard gray images 'Lena', 'F16', and 'Peppers' in the field of image processing as typical test objects, and by comparing our proposed algorithm with the conventional algorithm and the popular STC representation algorithm for computing the lower order moments, the theoretical and experimental results presented in this paper show that the average execution time improvement ratios of the proposed NAMES approach over the STC approach, and also the conventional approach are 26.63%, and 82.57% respectively while maintaining the image quality.

Keywords moment computation, gray image representation, Gouraud shading method, non-symmetry and anti-packing model (NAM), S-Tree coding (STC)

Received March 17, 2010; accepted June 27, 2010

E-mail: zhengyp@scut.edu.cn

1 Introduction

Image representations have been widely applied in computer visualization, robotics, computer graphics, image processing, and pattern recognition. An efficient image representation can save space and facilitate the manipulation of the acquired images [1–3]. Based on the B-tree triangular coding (BTTC) method, Distasi et al. first proposed the spatial data structure (SDS) for representing gray images [4]. Later, a new S-Tree coding (STC) method using the S-Tree data structure [5] and the Gouraud shading approach [6] for image representation was proposed in [7]. Inspired by the concept of the packing problem, Chen et al. presented a novel non-symmetry and anti-packing model (NAM) for image representation in order to represent the image pattern more effectively [8]. Recently, by extending the popular Gouraud shading approach, we have proposed a novel image compression algorithm using the NAM and the extended shading (NAMES) representation approach [9]. Similar to the results achieved by using the BTTC method [4] and by using the STC method [7], the encoding of NAMES can be performed in $O(n\log n)$ time and the decoding can be performed in $O(n)$ time, where n denotes the number of pixels in a gray image. However, by comparing our proposed NAMES method with the popular STC method, the experimental results show that the former can significantly reduce the number of homogenous blocks and simultaneously has a lower bit rate than the latter while retaining satisfactory image quality [9].

Representing and manipulating images are two important issues in the fields of computer graphics, image processing, and pattern recognition [10–12]. Computing moments on the image is very important in the field of image processing [13–15]. The lower order moments are especially useful in many applications such as acquiring motion parameters [16], moment-preserving thresholding [17], deskewing rotationally symmetric shapes [18], and recognizing patterns by moment invariants [19]. Lately, based on the STC method, an efficient image algorithm for lower order moment computation (which can be performed in $O(K)$ time where K denotes the number of partitioned blocks) was proposed [20].

In this paper, by using the NAMES representation approach for gray images, we propose a fast algorithm for computing the lower order moments, which takes $O(N)$ time where N is the number of NAM blocks. By taking three idiomatic standard gray images 'Lena', 'F16', and 'Peppers' in the field of image processing as typical test objects, and by comparing our proposed algorithm with the popular block representation algorithm for computing the lower order moments [20], the theoretical and experimental results presented in this paper demonstrate the computational advantages of our proposed algorithm.

Section 2 presents the NAMES representation approach for gray images. In Section 3, we demonstrate how to compute the lower order moments efficiently on our proposed NAMES representation. In Section 4, some experiments are performed to demonstrate the computational advantages of the NAMES representation. Finally, some concluding remarks and ideas for future work are addressed in Section 5.

2 NAMES representation approach of gray images

In this section, we first introduce the Gouraud shading approach, which is one of the most popular smooth shading algorithms. And then, we present our extended Gouraud shading approach. Finally, we simply describe our NAMES representation approach of gray images. However, a more detailed description is presented in our recent work [9].

2.1 Gouraud shading approach

For convenience, a homogeneous subimage is called a homogeneous block. The formal definition of a homogeneous block B is shown in Fig. 1 where f_1, f_2, f_3, and f_4 are gray values of the four corners.

In the encoding phase and the decoding phase, the

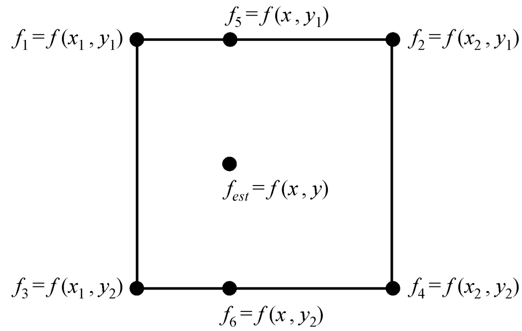

Fig. 1 Sketch of a homogeneous block B

Gouraud shading approach is used to control the image quality under a specified error tolerance. Given a specified error tolerance ε, a block is called a homogeneous block if the condition $|f(x,y)-f_{est}(x,y)|\leqslant\varepsilon$ holds for all the pixels in the block, where $f(x, y)$ is the gray value at the coordinate (x, y), $x_1\leqslant x\leqslant x_2$ and $y_1\leqslant y\leqslant y_2$.

By using the Gouraud shading method, i.e., linear interpolation, the estimated gray value at the coordinate (x, y) in the block is calculated by

$$f_{est}(x,y) = f_5 + (f_6-f_5) \times i_1, \tag{1}$$

where $f_5=f_1+(f_2-f_1)\times i_2$, $f_6=f_3+(f_4-f_3)\times i_2$, $i_1=(y-y_1)/(y_2-y_1)$, $i_2=(x-x_1)/(x_2-x_1)$, $x_1 < x_2$, and $y_1 < y_2$.

2.2 Extended the Gouraud shading approach

As far as the types of the NAM blocks are concerned, they may include four kinds of subpatterns, rectangles, horizontal line segments, vertical line segments, and isolated points. However, according to Eq. (1), it can be easily deduced that if $x_1 = x_2$ or $y_1 = y_2$, the value of i_2 or i_1 will be infinite. In these cases, it is obvious that we cannot obtain the estimated gray value $f_{est}(x, y)$ at the coordinate (x, y) in the block. Therefore, only the rectangle subpattern with the conditions $x_1 < x_2$, and $y_1 < y_2$ can utilize the Gouraud shading approach, and that the other three kinds of subpatterns cannot.

In the following paragraphs, by extending Eq. (1), we present how the other three kinds of subpattern calculate $f_{est}(x,y)$.

Case 1 $x_1\neq x_2$ and $y_1 = y_2$

In this case, a NAM block B is called a horizontal line segment subpattern and we extend Eq. (1) as follows

$$f_{est}(x,y) = f_1 + (f_4-f_1) \times i_2, \tag{2}$$

where $i_2 = (x - x_1)/(x_2 - x_1)$.

Case 2 $x_1 = x_2$ and $y_1 \neq y_2$

In this case, a NAM block B is called a vertical line segment subpattern and we extend the Eq. (1) as follows

$$f_{est}(x,y) = f_1 + (f_4 - f_1) \times i_1, \tag{3}$$

where $i_1 = (y - y_1)/(y_2 - y_1)$.

Case 3 $x_1 = x_2$ and $y_1 = y_2$

In this case, a NAM block B is called an isolated point subpattern and we extend the Eq. (1) as follows

$$f_{est}(x,y) = f_1. \tag{4}$$

2.3 A simple example of the NAMES representation approach of gray images

The following Fig. 2 illustrates the NAMES representation approach. Fig. 2(a) is a subimage of Lena's left eye with size 16×16 cut from Fig. 3(a). According to the NAM decomposition rule under the error tolerance $\varepsilon = 20$, Fig. 2(b) denotes the partitioned homogeneous blocks of Fig. 2(a).

It can be seen in Fig. 2(b) that 24 NAM blocks are needed to represent the original image, 18 rectangles, 2 horizontal line segments, 4 vertical line segments, and 0 isolated points. The peak signal to noise ratio ($PSNR$) of the reconstructed image is 30.7308 according to the following equation:

$$PSNR = 10\log_{10}\frac{255^2 \times M^2}{\sum_{x=0}^{M-1}\sum_{y=0}^{M-1}[f(x,y) - f_{est}(x,y)]^2},$$

where f is a given gray image of size $M \times M$ and f_{est} is a reconstructed image with a specified error tolerance ε. However, if the STC approach is used for partitioning, 31 rectangular blocks are needed to represent the original image and the $PSNR$ of the reconstructed image is 32.5174. Therefore, by comparing our proposed NAMES approach with the popular STC approach, the experimental results show that the former can reduce the number of homogenous blocks by 22.58% than the latter whereas retaining satisfactory image quality, whose $PSNR$ is still higher than 30.

100	103	100	96	74	75	73	67	82	73	81	59	54	47	56	81
69	70	87	84	64	64	67	62	57	59	57	54	50	44	50	53
60	52	59	64	56	54	57	53	50	56	49	50	53	51	53	53
53	51	54	52	51	52	52	49	50	47	49	48	46	50	59	48
50	53	52	52	58	51	47	50	52	46	48	46	47	44	51	55
53	53	51	53	55	51	53	45	44	42	47	46	47	48	79	66
48	48	47	55	47	51	48	46	44	46	47	44	50	56	70	90
48	53	53	47	43	54	49	50	40	46	48	76	62	69	94	128
61	77	67	43	47	62	60	45	39	36	40	88	87	65	86	121
82	90	81	50	60	80	79	48	38	36	39	56	90	65	50	72
92	103	90	50	57	94	93	76	48	41	43	69	112	77	56	66
95	115	107	71	52	92	98	90	72	66	66	90	108	74	53	87
93	117	121	99	67	58	84	98	86	86	91	83	72	57	66	126
90	108	127	115	88	59	60	79	87	90	80	77	55	65	113	173
92	105	114	125	113	89	62	57	54	61	58	65	77	107	160	198
99	113	112	117	120	113	95	82	63	66	75	88	127	158	188	202

(a)

100	103	100	96	74	75	73	67	82	73	81	59	54	47	56	81
69	70	87	84	64	64	67	62	57	59	57	54	50	44	50	53
60	52	59	64	56	54	57	53	50	56	49	50	53	51	53	53
53	51	54	52	51	52	52	49	50	47	49	48	46	50	59	48
50	53	52	52	58	51	47	50	52	46	48	46	47	44	51	55
53	53	51	53	55	51	53	45	44	42	47	46	47	48	79	66
48	48	47	55	47	51	48	46	44	46	47	44	50	56	70	90
48	53	53	47	43	54	49	50	40	46	48	76	62	69	94	128
61	77	67	43	47	62	60	45	39	36	40	88	87	65	86	121
82	90	81	50	60	80	79	48	38	36	39	56	90	65	50	72
92	103	90	50	57	94	93	76	48	41	43	69	112	77	56	66
95	115	107	71	52	92	98	90	72	66	66	90	108	74	53	87
93	117	121	99	67	58	84	98	86	86	91	83	72	57	66	126
90	108	127	115	88	59	60	79	87	90	80	77	55	65	113	173
92	105	114	125	113	89	62	57	54	61	58	65	77	107	160	198
99	113	112	117	120	113	95	82	63	66	75	88	127	158	188	202

(b)

Fig. 2 An example of the NAMES approach. (a) A 16 × 16 digital subimage; (b) partitioned homogenous blocks of (a)

3 Proposed NAMES-based algorithm for computing the lower order moments

In this section, we propose a fast algorithm for computing the lower order moments on the NAMES representation, which takes $O(N)$ time where N is the number of NAM blocks. Given an $M \times M$ image, let $f(x, y)$ denote the gray value of the pixel at the coordinate (x, y) for $0 \leqslant x$ and $y \leqslant M - 1$. The $(p + q)$th order moment is defined as follows

$$m_{pq} = \sum_{x=0}^{M-1}\sum_{y=0}^{M-1} x^p y^q f(x,y). \tag{5}$$

Suppose that a gray image of size $M \times M$ has been decomposed into the NAMES representation where the number of NAM blocks is N, and that the upper-left and the lower-right coordinates of the ith NAM block B_i are

(x_{1i}, y_{1i}) and (x_{2i}, y_{2i}), respectively. Let the width, W_i, and the height, H_i, of NAM block B_i be $(W_i = x_{2i}-x_{1i}+1)$ and $(H_i = y_{2i}-y_{1i}+1)$, respectively. By using NAM and the extended Gouraud approach, we first present a new Theorem 1 for computing the NAM block B_i in $O(1)$ time. This proposed theorem 1 is an extension of our previous theory which was presented in [8], and which only can deal with rectangular subpatterns with the conditions $x_{1i} < x_{2i}$ and $y_{1i} < y_{2i}$. Our new proposed Theorem 1 can not only deal with the rectangular subpattern but also can deal with all three other kinds of subpattern with the conditions $x_{1i} = x_{2i}$ or $y_{1i} = y_{2i}$. Then, we further present Theorem 2 which demonstrates that the NAMES representation can compute the estimated lower order moments in $O(N)$ time.

Theorem 1 *The estimated lower order moments of the* ith *NAM block* B_i, *i.e.*, m_{pqi}, *where* $0 \leqslant p+q \leqslant 3$, *can be calculated in* $O(1)$ *time*.

Proof According to the proposed NAMES approach, Eq. (5) can be rewritten as follows

$$m_{pq} = \sum_{i=1}^{N} m_{pqi} = \sum_{i=1}^{N}\sum_{x=0}^{W_i-1}\sum_{y=0}^{H_i-1}(x+x_{1i})^p(y+y_{1i})^q f_{est}(x+x_{1i}, y+y_{1i}). \tag{6}$$

From Eq. (6), we know that

$$\begin{aligned} m_{pqi} &= \sum_{x=0}^{W_i-1}\sum_{y=0}^{H_i-1}(x+x_{1i})^p(y+y_{1i})^q f_{est}(x+x_{1i}, y+y_{1i}) \\ &= \sum_{x=0}^{W_i-1}\sum_{y=0}^{H_i-1}\left[\left(x^p + C_p^1 x^{p-1}x_{1i} + \cdots + x_{1i}^p\right)\right. \\ &\quad \times \left(y^q + C_q^1 y^{q-1}y_{1i} + \cdots + y_{1i}^q\right) \\ &\quad \left.\times f_{est}(x+x_{1i}, y+y_{1i})\right] \\ &= \sum_{x=0}^{W_i-1}\sum_{y=0}^{H_i-1} x^p y^q f_{est}(x+x_{1i}, y+y_{1i}) \\ &\quad + C_q^1 y_{1i}\sum_{x=0}^{W_i-1}\sum_{y=0}^{H_i-1} x^p y^{q-1} f_{est}(x+x_{1i}, y+y_{1i}) + \cdots \\ &\quad + y_{1i}^q \sum_{x=0}^{W_i-1}\sum_{y=0}^{H_i-1} x^p f_{est}(x+x_{1i}, y+y_{1i}) \\ &\quad + C_p^1 x_{1i}\sum_{x=0}^{W_i-1}\sum_{y=0}^{H_i-1} x^{p-1} y^q f_{est}(x+x_{1i}, y+y_{1i}) \\ &\quad + C_q^1 C_p^1 x_{1i} y_{1i}\sum_{x=0}^{W_i-1}\sum_{y=0}^{H_i-1} x^{p-1} y^{q-1} f_{est}(x+x_{1i}, y+y_{1i}) + \cdots \\ &\quad + C_p^1 x_{1i} y_{1i}^q \sum_{x=0}^{W_i-1}\sum_{y=0}^{H_i-1} x^{p-1} f_{est}(x+x_{1i}, y+y_{1i}) + \cdots \\ &\quad + x_{1i}^p \sum_{x=0}^{W_i-1}\sum_{y=0}^{H_i-1} y^q f_{est}(x+x_{1i}, y+y_{1i}) \\ &\quad + C_q^1 x_{1i}^p y_{1i}\sum_{x=0}^{W_i-1}\sum_{y=0}^{H_i-1} y^{q-1} f_{est}(x+x_{1i}, y+y_{1i}) + \cdots \\ &\quad + x_{1i}^p y_{1i}^q \sum_{x=0}^{W_i-1}\sum_{y=0}^{H_i-1} f_{est}(x+x_{1i}, y+y_{1i}), \end{aligned} \tag{7}$$

where $C_n^r = \dfrac{n!}{r!(n-r)!}$.

We can notice that the key computation in above Eq. (7) is

$$T_{pqi} = \sum_{x=0}^{W_i-1}\sum_{y=0}^{H_i-1} x^p y^q f_{est}(x+x_{1i}, y+y_{1i}). \tag{8}$$

By using the extended Gouraud shading approach, the estimated gray value at the coordinate $(x+x_{1i}, y+y_{1i})$, i.e., $f_{est}(x+x_{1i}, y+y_{1i})$, can be calculated according to the type of the NAM block B_i, where $0 \leqslant x \leqslant W_i-1$ and $0 \leqslant y \leqslant H_i-1$. Therefore, in terms of the values of the coordinates (x_{1i}, y_{1i}) and (x_{2i}, y_{2i}), the following four cases are considered.

Case 1 $x_{1i} < x_{2i}$ and $y_{1i} < y_{2i}$

$f_{est}(x+x_{1i}, y+y_{1i}) = f_{1i} + Ax + By + Cxy$, where $A = (f_{2i}-f_{1i})/(W_i-1)$, $B = (f_{3i}-f_{1i})/(H_i-1)$, and $C = (f_{1i}-f_{2i}-f_{3i}+f_{4i})/((W_i-1)(H_i-1))$. We can rewrite Eq. (8) as follows

$$\begin{aligned} T_{pqi} &= \sum_{x=0}^{W_i-1}\sum_{y=0}^{H_i-1} x^p y^q f_{est}(x+x_{1i}, y+y_{1i}) \\ &= \sum_{x=0}^{W_i-1}\sum_{y=0}^{H_i-1} x^p y^q (f_{1i} + Ax + By + Cxy) \\ &= f_{1i}\sum_{x=0}^{W_i-1}\sum_{y=0}^{H_i-1} x^p y^q + A\sum_{x=0}^{W_i-1}\sum_{y=0}^{H_i-1} x^{p+1} y^q \\ &\quad + B\sum_{x=0}^{W_i-1}\sum_{y=0}^{H_i-1} x^p y^{q+1} + C\sum_{x=0}^{W_i-1}\sum_{y=0}^{H_i-1} x^{p+1} y^{q+1} \\ &= f_{1i}\sum_{x=0}^{W_i-1} x^p \sum_{y=0}^{H_i-1} y^q + A\sum_{x=0}^{W_i-1} x^{p+1}\sum_{y=0}^{H_i-1} y^q \\ &\quad + B\sum_{x=0}^{W_i-1} x^p \sum_{y=0}^{H_i-1} y^{q+1} + C\sum_{x=0}^{W_i-1} x^{p+1}\sum_{y=0}^{H_i-1} y^{q+1}. \end{aligned} \tag{9}$$

In Eq. (9), let $g(u,v)=\sum_{x=0}^{u-1}x^v$, then the summation $g(W_i,p)=\sum_{x=0}^{W_i-1}x^p$ for a specific p, where $0\leqslant p\leqslant 4$, can be computed in $O(1)$ time by using the following five separated equations [8,11].

$$g(W_i,0)=\sum_{x=0}^{W_i-1}x^0=W_i,$$
$$g(W_i,1)=\sum_{x=0}^{W_i-1}x^1=\frac{W_i(W_i-1)}{2},$$
$$g(W_i,2)=\sum_{x=0}^{W_i-1}x^2=\frac{W_i(W_i-1)(2W_i-1)}{6},$$
$$g(W_i,3)=\sum_{x=0}^{W_i-1}x^3=\frac{W_i^2(W_i-1)^2}{4},$$
$$g(W_i,4)=\sum_{x=0}^{W_i-1}x^4=\frac{W_i(W_i-1)(2W_i-1)(3W_i^2-3W_i-1)}{30}.$$

Similarly, the summation $g(H_i,q)=\sum_{x=0}^{H_i-1}x^q$ for a specific q, where $0\leqslant q\leqslant 4$, can also be computed in $O(1)$ time. Therefore, we can obtain the following Eq. (10)

$$\begin{aligned}T_{pqi}=&f_{1i}\sum_{x=0}^{W_i-1}x^p\sum_{y=0}^{H_i-1}y^q+A\sum_{x=0}^{W_i-1}x^{p+1}\sum_{y=0}^{H_i-1}y^q\\&+B\sum_{x=0}^{W_i-1}x^p\sum_{y=0}^{H_i-1}y^{q+1}+C\sum_{x=0}^{W_i-1}x^{p+1}\sum_{y=0}^{H_i-1}y^{q+1}\\=&f_{1i}g(W_i,p)g(H_i,q)+Ag(W_i,p+1)g(H_i,q)\\&+Bg(W_i,p)g(H_i,q+1)\\&+Cg(W_i,p+1)g(H_i,q+1).\end{aligned}\tag{10}$$

Case 2 $x_{1i}\neq x_{2i}$ and $y_{1i}=y_{2i}$

$f_{est}(x+x_{1i},y+y_{1i})=f_{1i}+Ax$, where $A=(f_{2i}-f_{1i})/(W_i-1)$. We can rewrite Eq. (8) as follows

$$\begin{aligned}T_{pqi}&=\sum_{x=0}^{W_i-1}\sum_{y=0}^{H_i-1}x^py^qf_{est}(x+x_{1i},y+y_{1i})\\&=\sum_{x=0}^{W_i-1}\sum_{y=0}^{H_i-1}x^py^q(f_{1i}+Ax)\\&=f_{1i}\sum_{x=0}^{W_i-1}\sum_{y=0}^{H_i-1}x^py^q+A\sum_{x=0}^{W_i-1}\sum_{y=0}^{H_i-1}x^{p+1}y^q\\&=f_{1i}\sum_{x=0}^{W_i-1}x^p\sum_{y=0}^{H_i-1}y^q+A\sum_{x=0}^{W_i-1}x^{p+1}\sum_{y=0}^{H_i-1}y^q\\&=f_{1i}g(W_i,p)g(H_i,q)+Ag(W_i,p+1)g(H_i,q).\end{aligned}\tag{11}$$

Case 3 $x_{1i}=x_{2i}$ and $y_{1i}\neq y_{2i}$

$f_{est}(x+x_{1i},y+y_{1i})=f_{1i}+By$, where $B=(f_{3i}-f_{1i})/(H_i-1)$. We can rewrite Eq. (8) as follows

$$\begin{aligned}T_{pqi}&=\sum_{x=0}^{W_i-1}\sum_{y=0}^{H_i-1}x^py^qf_{est}(x+x_{1i},y+y_{1i})\\&=\sum_{x=0}^{W_i-1}\sum_{y=0}^{H_i-1}x^py^q(f_{1i}+By)\\&=f_{1i}\sum_{x=0}^{W_i-1}\sum_{y=0}^{H_i-1}x^py^q+B\sum_{x=0}^{W_i-1}\sum_{y=0}^{H_i-1}x^py^{q+1}\\&=f_{1i}\sum_{x=0}^{W_i-1}x^p\sum_{y=0}^{H_i-1}y^q+B\sum_{x=0}^{W_i-1}x^p\sum_{y=0}^{H_i-1}y^{q+1}\\&=f_{1i}g(W_i,p)g(H_i,q)+Bg(W_i,p)g(H_i,q+1).\end{aligned}\tag{12}$$

Case 4 $x_{1i}=x_{2i}$ and $y_{1i}=y_{2i}$

$f_{est}(x+x_{1i},y+y_{1i})=f_{1i}$. We can rewrite Eq. (8) as follows

$$\begin{aligned}T_{pqi}&=\sum_{x=0}^{W_i-1}\sum_{y=0}^{H_i-1}x^py^qf_{est}(x+x_{1i},y+y_{1i})\\&=\sum_{x=0}^{W_i-1}\sum_{y=0}^{H_i-1}x^py^qf_{1i}\\&=f_{1i}\sum_{x=0}^{W_i-1}\sum_{y=0}^{H_i-1}x^py^q\\&=f_{1i}\sum_{x=0}^{W_i-1}x^p\sum_{y=0}^{H_i-1}y^q\\&=f_{1i}g(W_i,p)g(H_i,q).\end{aligned}\tag{13}$$

The previous Eqs. (10)–(13) imply that the computation of T_{pqi} can be performed in $O(1)$ time for the above four cases, and the moments m_{pqi}, where $0\leqslant p+q\leqslant 3$, can also be computed in $O(1)$ time.

The proof is completed hereon.

From Theorem 1 and Eq. (6), we can easily obtain the following result presented in Theorem 2.

Theorem 2 *Suppose a gray image of size $M\times M$ has been represented by using the NAMES approach with N blocks, the estimated lower order moments on the NAMES representation can be computed in $O(N)$ time.*

As far as the STC approach is concerned, since the bintree segmentation is symmetric, the segmentation method suffers from a great confine. However, since the

NAMES segmentation is asymmetrical, the segmentation method is unrestricted. The purpose of the NAMES segmentation is to construct subpatterns as large as possible and yield the fewest subpatterns number for a packed pattern. Generally speaking, the total number of subpatterns of the NAMES, say N, is less than the total number of nodes of the STC, say K, i.e., $N < K$. Since the computation complexity of the estimated lower order moments on the STC representation is $O(K)$, it follows that the NAMES approach can compute the estimated lower order moments faster than the STC approach.

4 Experimental results

Before describing and analyzing the experimental results, we first reintroduce a definition of the complexity of an image [8], which reflects how complex an image is.

Definition 1 *The complexity of an image is defined as follows*

$$C = N_{LQT}/N_f,$$

where N_{LQT} is the total number of nodes in the image which is represented by the method of the linear quadtree and N_f is the size of the image.

Since N_{LQT} is no greater than N_f, we know that $0 < C \leqslant 1$. In addition, the larger the value of C, the more complex the image.

Fig. 3 Three idiomatic standard gray images. (a) Lena; (b) F16; (c) Peppers

In this section, all our experiments are performed on a Celeron microprocessor running at 2.4 GHz with 2 GB RAM. The operating system is MS-Windows XP running the Matlab 7.0 environment. Three idiomatic standard gray images, each of size 512 × 512 are shown in Fig. 3 and are used as the benchmark to evaluate the performance of moment computation for the conventional approach, the previous STC approach, and our proposed NAMES approach. Since the representation method of NAMES is adaptable to all kinds of texture images and our proposed method for computing the moment in this paper is based on the NAMES representation method, the proposed method works well with texture rich images.

Given six values of error tolerances ε = 5, 10, 15, 20, 25, and 30, Table 1 lists the complexity of a gray image C,

Table 1 Comparison of number of blocks between NAMES and STC

Image	C	ε	Number of blocks		ΔN/%
			STC	NAMES	
Lena	0.9970	5	41242	36202	12.22
		10	19821	17370	12.37
		15	12977	10687	17.65
		20	9428	7686	18.48
		25	7210	5898	18.20
		30	5676	4693	17.32
F16	0.9864	5	33579	28584	14.88
		10	20725	15559	24.93
		15	15698	10548	32.81
		20	12594	8016	36.35
		25	10321	6513	36.90
		30	8637	5356	37.99
Peppers	0.9988	5	50871	45287	10.98
		10	25255	22902	9.32
		15	14457	12540	13.26
		20	10235	7984	21.99
		25	8061	5924	26.51
		30	6616	4770	27.90

which was defined in our previous work [8], the number of homogenous blocks N for both the NAMES method and the STC method, and $\Delta N = (N(\mathrm{STC}) - N(\mathrm{NAMES}))/N(\mathrm{STC})$. The three images have different image complexities, which reflect how complex these images are. From Table 1, we can easily notice that the number of blocks in NAMES is always less than that in STC. In fact, further comparison of the number of homogenous blocks in each method, allows us to calculate that the NAMES can significantly reduce the number of homogenous blocks by 12.22%–18.48%, 14.88%–37.99%, and 9.32%–27.90% over STC in pictures 'Lena', 'F16', and 'Peppers', respectively (see Figs. 3(a)–(c)).

To corroborate our theoretical results obtained in Section 3, we evaluate the execution time performance of the three representation approaches by applying the NAMES approach, the STC approach, and the conventional approach to moment computation.

Table 2 demonstrates the moment accuracy comparison of the three approaches for an error tolerance $\varepsilon = 20$. We notice that the estimated moments calculated by the NAMES approach are very close to the estimated moments computed by the STC approach. Also, we notice that the moments calculated by the NAMES method are satisfactory when compared to the exact moments calculated by the conventional method running on the original input gray image. For example, as far as the image 'Lena' is concerned, the estimated moments of m_{12} calculated by the STC approach and the NAMES approach are 7.75E + 14 and 7.74E + 14, respectively and the exact moments calculated by the conventional method is 7.78E + 14.

Fig. 4 illustrates the execution time for the three approaches for 'Lena', 'F16', and 'Peppers', respectively. The time unit for the moment computation is milliseconds. From Fig. 4, we notice that, for all specified error tolerances, the execution time of the conventional approach for 'Lena', 'F16', and 'Peppers' is constant at 260.82, 357.23, and 298.58 ms, respectively. Also, it can be seen that the NAMES approach for computing lower order moments is always faster than the previous STC approach under the different error tolerances. For the error tolerance $\varepsilon = 20$, the execution time of the NAMES (STC) approach for 'Lena', 'F16', and 'Peppers' is 52.11 (63.28), 54.08 (85.02), and 53.63 (69.50) ms, respectively.

When $\varepsilon = 20$, it can be calculated that the proposed NAMES approach provides an average execution time improvement ratio of 26.63% over the STC approach. The average execution time improvement ratio of the proposed NAMES approach over the conventional approach is 82.57%.

Therefore, the experimental results in this section show that the NAMES approach for computing lower order moments is faster than the previous STC approach, which corroborates the theoretical results.

5 Conclusions

In this paper, inspired by the idea of computing moments on a block representation and using the NAM and extended Gouraud shading (NAMES) approach, we have proposed a fast algorithm for computing the lower order moments on the NAMES representation, which takes $O(N)$ time where N is the number of NAM blocks. By taking three idiomatic standard gray images 'Lena', 'F16', and 'Peppers' in the field of image processing as typical test objects, and by comparing our proposed algorithm with the popular block representation algorithm for computing the lower order moments, the theoretical and

Table 2 Accuracy comparison of moment among the three approaches

	Conventional approach			STC approach			NAMES approach		
	Lena	F16	Peppers	Lena	F16	Peppers	Lena	F16	Peppers
m_{00}	3.25E + 07	4.70E + 07	2.73E + 07	3.23E + 07	4.68E + 07	2.73E + 07	3.23E + 07	4.67E + 07	2.72E + 07
m_{10}	8.08E + 09	1.19E + 10	6.77E + 09	8.06E + 09	1.18E + 10	6.77E + 09	8.06E + 09	1.17E + 10	6.75E + 09
m_{01}	8.70E + 09	1.23E + 10	7.11E + 09	8.66E + 09	1.23E + 10	7.10E + 09	8.65E + 09	1.21E + 10	7.08E + 09
m_{11}	2.20E + 12	3.08E + 12	1.69E + 12	2.20E + 12	3.07E + 12	1.69E + 12	2.19E + 12	3.06E + 12	1.69E + 12
m_{20}	2.71E + 12	4.05E + 12	2.28E + 12	2.71E + 12	4.04E + 12	2.28E + 12	2.71E + 12	4.04E + 12	2.27E + 12
m_{02}	3.03E + 12	4.27E + 12	2.44E + 12	3.02E + 12	4.26E + 12	2.44E + 12	3.02E + 12	4.24E + 12	2.43E + 12
m_{21}	7.45E + 14	1.04E + 15	5.51E + 14	7.42E + 14	1.04E + 15	5.51E + 14	7.40E + 14	1.03E + 15	5.50E + 14
m_{12}	7.78E + 14	1.07E + 15	5.64E + 14	7.75E + 14	1.07E + 15	5.64E + 14	7.74E + 14	1.06E + 15	5.63E + 14
m_{30}	1.03E + 15	1.57E + 15	8.71E + 14	1.03E + 15	1.56E + 15	8.69E + 14	1.03E + 15	1.55E + 15	8.67E + 14
m_{03}	1.17E + 15	1.66E + 15	9.43E + 14	1.17E + 15	1.66E + 15	9.41E + 14	1.16E + 15	1.66E + 15	9.41E + 14

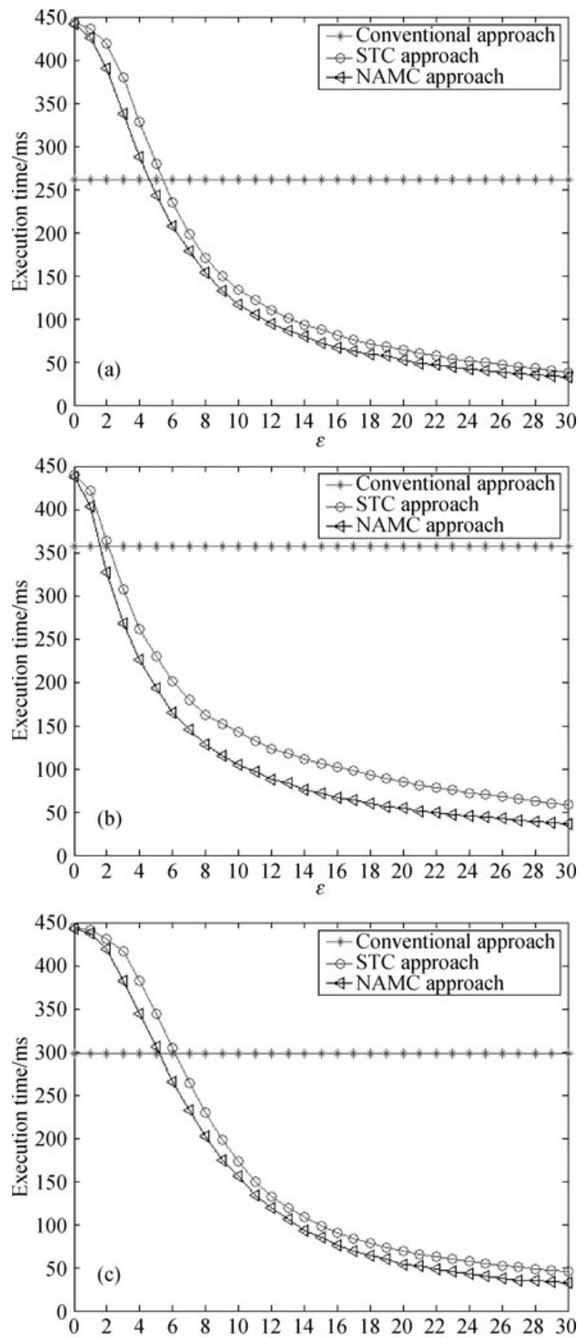

Fig. 4 Performance comparisons between conventional, STC, and NAMES approaches for (a) ‘Lena’; (b) ‘F16’; (c) ‘Peppers’

experimental results presented in this paper demonstrate the computational advantage of our proposed algorithm.

In the future, we will consider designing some other NAMES-based image manipulations, such as neighbor finding, area computing, and set operations, since an efficient image representation can not only save space but also facilitate the manipulation of the acquired images.

Acknowledgements The authors wish to acknowledge the support of the National High Technology Research and Development Program of China (863 Program) (2006AA04Z211) and the National Natural Science Foundation of China (Grant No. 60973085).

References

1. Tanaka Y, Ikehara M, Nguyen T Q. Multiresolution image representation using combined 2-D and 1-D directional filter banks. IEEE Transactions on Image Processing, 2009, 18(2): 269–280
2. Guo J M, Wu M F. Improved block truncation coding based on the void-and-cluster dithering approach. IEEE Transactions on Image Processing, 2009, 18(1): 211–213
3. Yang E H, Wang L. Joint optimization of run-length coding, Huffman coding, and quantization table with complete baseline JPEG decoder compatibility. IEEE Transactions on Image Processing, 2009, 18(1): 63–74
4. Distasi R, Nappi M, Vitulano S. Image compression by B-tree triangular coding. IEEE Transactions on Communications, 1997, 45(9): 1095–1100
5. Dejonge W, Scheuermann P, Schijf A. S+-Trees: an efficient structure for the representation of large pictures. Computer Vision and Image Understanding, 1994, 59(3): 265–280
6. Foley J D, Dam A V, Feiner S K, Hughes J F. Computer Graphics, Principle, and Practice. 2nd ed. Reading: Addision-Wesley, 1990
7. Chung K L, Wu J G. Improved image compression using S-tree and shading approach. IEEE Transactions on Communications, 2000, 48(5): 748–751
8. Chen C B, Zheng Y P, Sarem M. A novel non-symmetry and anti-packing model for image representation. Chinese Journal of Electronics, 2009, 18(1): 89–94
9. Zheng Y, Chen C. Study on a new algorithm for gray image representation. Chinese Journal of Computers, 2010 (in press)
10. Qiao Y, Wang W, Minematsu N, Liu J, Takeda M, Tang X. A theory of phase singularities for image representation and its applications to object tracking and image matching. IEEE Transactions on Image Processing, 2009, 18(10): 2153–2166
11. Chung K L, Liu Y W, Yan W M. A hybrid gray image representation using spatial- and DCT-based approach with application to moment computation. Journal of Visual Communication and Image Representation, 2006, 17(6): 1209–1226
12. Chung K L, Yan W M, Liao Z H. Fast computation of moments on compressed grey images using block representation. Real-Time Imaging, 2002, 8(2): 137–144
13. Papakostas G A, Boutalis Y S, Karras D A, Mertzios B G. Fast numerically stable computation of orthogonal Fourier-Mellin moments. IET Computer Vision, 2007, 1(1): 11–16

14. Kotoulas L, Andreadis I. Fast computation of Chebyshev moments. IEEE Transactions on Circuits and Systems for Video Technology, 2006, 16(7): 884–888
15. Kotoulas L, Andreadis I. Accurate calculation of image moments. IEEE Transactions on Image Processing, 2007, 16(8): 2028–2037
16. Pei S C, Liou L G. Using moments to acquire the motion parameters of a deformable object without correspondences. Image and Vision Computing, 1994, 12(8): 475–485
17. Tsai W H. Moment-preserving thresholding: a new approach. Computer Vision Graphics and Image Processing, 1985, 29(3): 377–393
18. Pei S C, Horng J H. A moment-based approach for deskewing rotationally symmetric shapes. IEEE Transactions on Image Processing, 1999, 8(12): 1831–1834
19. Lin H, Si J, Abousleman G P. Orthogonal rotation-invariant moments for digital image processing. IEEE Transactions on Image Processing, 2008, 17(3): 272–282
20. Chung K, Chen P. An efficient algorithm for computing moments on a block representation of a grey-scale image. Pattern Recognition, 2005, 38(12): 2578–2586